

1 **SUPPLEMENTARY INFORMATION**

2
3 **SepF supports the recruitment of the DNA translocase SftA to the Z-ring**

4
5
6 Terrens N. V. Saaki, Zihao Teng, Michaela Wenzel, Magali Ventroux, Rut Carballido-López,
7 Marie Francoise Noirot-Gros, Leendert W. Hamoen

8
9
10 **Content:**

- 11 • General bacterial growth conditions
- 12 • Plasmid and strain construction
- 13 • Table S1: Strains used in this study
- 14 • Table S2: Plasmids used in this study
- 15 • Table S3: Primers used in this study
- 16 • Fig. S1 Secondary structure prediction of SftA using PSIPred
- 17 • Fig. S2: Localization of SftA in different cell division mutants
- 18 • Fig. S3: SftA recruitment does not depend on late cell division proteins
- 19 • Fig. S4: Large field microscopy images of mutants shown in Fig. 5.
- 20 • Fig. S5: SftA inhibits SepF ring formation
- 21 • Fig. S6: Assembly of FtsZ-rings over nucleoids
- 22 • References

25 **General bacterial growth conditions**

26 *E. coli* strain TOP10 was used for the construction and propagation of all plasmids. All *B.*
27 *subtilis* strains were derived from strain 168ca *trpC2* (Zeigler *et al.*, 2008). Strains were grown
28 at 37 °C in Lysogeny broth (LB) medium supplemented with antibiotics. For transformation,
29 *B. subtilis* was grown in minimal medium as described before (Hamoen *et al.*, 2006). Antibiotic
30 concentrations used were 100 µg/ml ampicillin, 5 µg/ml chloramphenicol, 5 µg/ml
31 kanamycin, 10 µg/ml tetracycline, 2 µg/ml phleomycin and 2 µg/ml erythromycin.

32 The PSIPRED secondary structure prediction method was used to predict secondary
33 structures in the SftA sequences (Jones, 1999). Two helices were found in the first 21 amino
34 acids sequence and Amphipaseek predicts the first one likely to be an amphipathic helix.

35

36 **Plasmid and strain construction**

37 Strains and plasmids used are listed in table S1 and S2, respectively. Relevant primers used
38 for cloning are shown in table S3. For cloning, either classical restriction or Gibson Assembly
39 was used (Gibson *et al.*, 2009). The deletion mutants of *sftA* (BKE29805, BKK29805) were
40 acquired from the Bacillus genomic stock centre (Koo *et al.*, 2017). Chromosomal DNA of
41 these strains was transformed into wild type *B. subtilis* 168 to achieve strains TNVS083
42 (*sftA::erm*) and TNVS825 (*sftA::kan*), respectively.

43 To localize SftA, YdeL and PsdS, we constructed strains TNVS455, TNVS366 and
44 TNVS810, respectively. To this end, the *sftA* gene was amplified with primers TerS279 and
45 TerS280 from *B. subtilis* 168 genomic DNA and Gibson assembled into plasmid pMW1 (Müller
46 *et al.*, 2016), linearized with primer pairs TerS153/TerS274, resulting in plasmid pTNV144
47 (*Pxyl-sftA-msfGFP*). This placed the *sftA-msfGFP* reporter under control of the xylose-
48 inducible *Pxyl* promoter. The primers added an affinity tag of 6 histidines to allow future
49 pulldown experiments, but this was not used in this manuscript. Next, plasmid pTNV144 was

50 transformed into TNVS83, resulting in strain TNVS455 (*sftA::erm P_{xyl}-sftA-msfGFP*). The *ydeL*
51 gene was amplified from *B. subtilis* 168 genomic DNA using primers TerS127 and TerS128.
52 The product was inserted into the *amyE* locus integration plasmid pSG1729 (Lewis and
53 Marston, 1999), using *XhoI* and *NotI* sites, resulting in plasmid pTNV022. Integration of
54 plasmid pTNV022 into wild type *B. subtilis* resulted in strain TNVS042. To construct a PsdS-
55 GFP fusion, first plasmid pTNV143 was created. The monomeric super-folder GFP variant from
56 pTNV064 (Müller *et al.*, 2016) was amplified using primers TerS283/TerS413 and Gibson
57 assembled into pSG1729, which was linearized with primers TerS274 and TerS414, resulting
58 in pTNV100. This plasmid contains no unwanted additional amino acids in the multiple cloning
59 site and can be used to tag proteins of interest at their C-termini with monomeric super folder
60 GFP. Subsequently, pTNV100 was linearized with primers TerS484 and TerS283 and
61 circularized using Gibson assembly, resulting in plasmid pTNV143 (*P_{xyl}-msfGFP*). The *psdS*
62 gene was amplified with primers TerS621 and TerS622 from *B. subtilis* 168 genomic DNA and
63 Gibson assembled into pTNV143 linearized with primers TerS274 and TerS368. The Gibson
64 assembly product was transformed directly into competent *B. subtilis* 168 cells, resulting in
65 strain TNVS810 (*P_{xyl}-psdS-msfgfp*). The fusion proteins were expressed from the xylose
66 inducible *P_{xyl}* promoter.

67 To test whether SftA is recruited to cell division site by the early or late cell division
68 proteins, two strains were constructed each harbouring the mCherry-ZapA and SftA-GFP
69 reporter fusions, and one containing IPTG-inducible *ftsZ* and the other IPTG-inducible *pbpB*.
70 *sftA* was amplified from *B. subtilis* genomic DNA with primers TerS001 and TerS002, which
71 adds a unique *ApaI* and *EcoRI* restriction site at each flank. Subsequently, the *ApaI* and *EcoRI*
72 digested product was inserted into linearized pSG1154 (Lewis and Marston, 1999), resulting
73 in plasmid pTNV001. This plasmid was transformed into competent *B. subtilis* 168 cells,
74 resulting in strain TNVS001 (*P_{xyl}-sftA-gfp*). To simultaneously express mCherry-ZapA and

75 SftA-GFP, competent cells of strain EKB36 (*zapA::Pxyl-mCherry-zapA*, kind gift from Edward
76 de Koning) was transformed with chromosomal DNA from strain TNVS001 (*Pxyl-sftA-gfp*),
77 resulting in strain TNVS353. To tightly control the expression of FtsZ and PbpB from the IPTG-
78 inducible *Pspac* promoter, an extra copy of the LacI repressor from strain DS7996 (*lacA::lacI*)
79 (Pozsgai *et al.*, 2011) was introduced into *B. subtilis* strain 168, resulting in strain TNVS209.
80 Chromosomal DNA of TNVS209 was used to transform competent cells of strain TNVS353
81 resulting in strain TNVS758. Inducible FtsZ was acquired by transforming chromosomal DNA
82 of strain 1801 (*ftsZ::Pspac-ftsZ*) (Marston *et al.*, 1998) into competent TNVS758, resulting in
83 strain TNVS786. To obtain the IPTG inducible PbpB strain, chromosomal DNA of strain 3294
84 (*chr::PdivIVA-gfp-divIVA Pspac-pbpB*) (Hamoen and Errington, 2003) was first transformed to
85 *B. subtilis* 168 cells to isolate the *Pspac-pbpB* locus, resulting in strain TNVS087 (*Pspac-pbpB*).
86 Finally, chromosomal DNA of strain TNVS87 was transformed into competent TNVS758,
87 resulting in strain TNVS783 (*Pxyl-mCherry-zapA Pxyl-sftA-gfp lacA::lacI Pspac-pbpB*).

88 To test whether amino acid residues 30 to 75 were required for recruitment of SftA,
89 SftA was first fused to GFP by amplifying the *sftA* gene from genomic DNA with primers
90 TerS279 and TerS280, and linearizing plasmid pMW1 (Müller *et al.*, 2016) with primers
91 TerS153 and TerS274, followed by Gibson assembly, resulting in plasmid pTNV063 (*Pxyl-sftA-*
92 *msfgfp*). A truncated variant of SftA comprising the first 149 amino acids was then
93 constructed. For this plasmid pTNV063 was PCR amplified with primer pairs TerS153 and
94 TerS145, and TerS203 and TerS146 to yield two separate products. These two products were
95 Gibson assembled to create plasmid pTNV069 (*Pxyl-sftA(M1-P149)-msfgfp*). Two different
96 PCR products with plasmid pTNV063 with primer pairs TerS153 and TerS145, and TerS203 and
97 TerS146, which were Gibson assembled, resulting in plasmid pTNV124 (*Pxyl-sftA(M1-P149)-*
98 *msfgfp*). Plasmid pTNV124 was transformed to competent cells of TNVS083 (*sftA::erm*)
99 resulting in strain TNVS456. Next, pTNV069 was also PCR amplified with primer pairs TerS180

100 and TerS342, and TerS179 and TerS341 to give two different products. Gibson assembly of
101 the two products removed the amino acids Q30 to R75 to yield plasmid pTNV093 (*PxyI-*
102 *sftA(M1-P149(Δ30-75))-msfgfp*). Plasmid pTNV093 was transformed to competent wild type
103 cells to result in strain TNVS224, and subsequent transformation of this strain with genomic
104 DNA from strain TNVS083 (*sftA::erm*) resulted in strain TNVS234.

105 To test whether the amphipathic helix of SftA is sufficient to target the protein to the
106 membrane, this helix was fused to monomeric GFP. To this end, plasmid pTNV124 (*PxyI-*
107 *sftA(M1-P149)-msfgfp*) was amplified with primer pairs TerS153 and TerS274, and TerS287
108 and TerS573, and Gibson assembled to obtain pTNV187 (*PxyI-sftA(M1-E14)-msfgfp*). This
109 plasmid was transformed into competent wild type cells, resulting in strain TNVS586.

110 To test which early cell division protein is important for SftA recruitment of a SftA
111 variant lacking the N-terminal amphipathic membrane targeting helix, plasmid pTNV144
112 (*PxyI-sftA-msfgfp*) was linearized with primer pair TerS274 and TerS282 followed by
113 subsequent recirculation using Gibson assembly, resulting in pTNV202 (*PxyI-sftAΔ(S2-E14)-*
114 *msfgfp*). This plasmid was then transformed into competent wild type cells, resulting in strain
115 TNVS729. To remove wild type *sftA*, genomic DNA of strain BKK29805 (Koo *et al.*, 2017) was
116 transformed into TNVS729. To evaluate the effect of different cell division proteins,
117 chromosomal DNA from either strain BFA2863 (*sepF::erm*) (Hamoen *et al.*, 2006), YK206
118 (*ftsA::erm*) (Ishikawa *et al.*, 2006), LH28 (*ezrA::cat*) (Gamba *et al.*, 2015), or 1356 (*zapA::tet*)
119 (Feucht and Errington, 2005) was transformed into competent TNVS947 cells, resulting in
120 strains TNVS949, TNVS950, TNVS951, and TNVS952, respectively.

121 To test whether FtsA is important for SftA recruitment, we constructed a minimal 61
122 amino acid long N-terminal domain that still showed some cell division localization activity by
123 PCR amplifying from plasmid pTNV063 (*PxyI-sftA-msfgfp*) using primer pair ZT189 and EKP22
124 followed by recircularization using Gibson assembly, resulting in plasmid pZH014 (*PxyI-*

125 *sftA(M1-P61)-msfgfp*). pZH014 was transformed into competent *B. subtilis* 168 cells, resulting
126 in strain TZh029. To remove wild type *sftA*, genomic DNA of strain BKK29805 (Koo *et al.*, 2017)
127 was transformed into TZh029 resulting in strain TZh035. To label the location of the Z-ring,
128 we amplified a fragment of *zapA::P_{xy}-mcherry-zapA-cat* from strain TNVS758 using primer pair
129 TerS314 and TerS315, then transformed this into TZh035, resulting in strain TZh119. To
130 evaluate the effect of a *sepF* or *ftsA* deletions, chromosomal DNA from either strain BFA2863
131 (*sepF::erm*) (Hamoen *et al.*, 2006) or TB07 (*ftsA::erm*), were transformed into competent
132 TZh119 cells, resulting in strains TZh120 and TZh121, respectively.

133 To determine the effect of an SftA null mutant on cell division in different cell division
134 mutants, we first introduced these mutations into the same *B. subtilis* 168 wild type
135 background. To this end genomic DNA from either a *zapA::tet* (strain 1356 (Feucht and
136 Errington, 2005)), *sepF::spc* (strain YK204 (Ishikawa *et al.*, 2006)), *ftsA::erm* (strain YK206)
137 (Ishikawa *et al.*, 2006) or *ezrA::spc* (strain PG049 (Gamba *et al.*, 2015)) strain was used to first
138 transform *B. subtilis* 168, resulting in strains TNVS193, TNVS159, TNVS281 and TNVS158,
139 respectively. Subsequently, *sftA* was deleted by introducing *sftA::erm* from TNVS083,
140 resulting in TNVS197, TNVS152 and TNVS171, respectively. Strain TNVS825 (*sftA::kan*) was
141 combined with YK206 (*ftsA::erm*) (Ishikawa *et al.*, 2006) to result in strain TNVS869 (*sftA::kan*
142 *ftsA::erm*).

143 To test whether overexpression of SftA affected cell division in the different cell
144 division mutants, the *amyE* locus integration plasmid pSG1729 (Lewis and Marston, 1999),
145 containing a xylose-inducible (P_{xy}) *gfp* gene, was PCR amplified to remove the *gfp* gene using
146 primer pairs TerS261 and TerS146, and TerS262 and TerS145. Ligation with Gibson assembly
147 resulted in plasmid pTNV061. We encountered some problems with the cloning in *E. coli* of
148 certain *sftA* containing plasmids, which was bypassed by utilizing a low copy number plasmid.
149 To achieve this, the low copy number origin pSC101 from plasmid pSEN29 (Genevaux *et al.*,

150 2004) was amplified with primer pair TerS478 and TerS479, to replace the ORI of plasmid
151 pTNV061 by PCR using primer pair TerS226 and TerS382. The two PCR products were Gibson
152 assembled to form the low copy number plasmid pTNV122. To introduce the *sftA* gene, the
153 plasmid was PCR linearized using primer pair TerS263 and TerS274, and the *sftA* gene was
154 amplified with primer pair TerS279 and TerS357. Gibson assembly of both PCR products
155 resulted in plasmid pTNV125 (*P_{xyl}-sftA*), which was subsequently integrated into the *amyE*
156 locus of wild type *B. subtilis* 168, resulting in strain TNVS390. TNVS390 was transformed with
157 chromosomal DNA from strains LH028 (*ezrA::cat*), BFA2863 (*sepF::erm*), 1356 (*zapA::tet*) and
158 YK206 (*ftsA::erm*), resulting in TNVS591, TNVS605, TNVS606 and TNVS622, respectively.

159 To test the effect of overexpression of the amino acid 1-149 N-terminal domain of SftA
160 on viability, this fragment was amplified with primer pair TerS279 and AH002 from genomic
161 DNA of *B. subtilis* 168 and cloned into the *amyE* integration plasmid pTNV143 linearized with
162 primer pair TerS274 and AH001, using Gibson assembly. The resulting plasmid pTNV166 was
163 transformed to *B. subtilis* 168, resulting in strain TNVS541 (*P_{xyl}-sftA(M1-P149)*). Strain
164 TNVS541 was transformed with chromosomal DNA of LH028 (Gamba *et al.*, 2015) containing
165 the *ezrA::cat* deletion resulting in strain TNVS602. The N-terminal domain of SftA was
166 overproduced by the addition of xylose.

167 To test whether SftA overexpression in $\Delta ezrA$ cells influenced Z-ring formation or the
168 recruitment of late cell division proteins, firstly, the spectinomycin marker of strain TNVS390
169 was replaced with the kanamycin marker of plasmid pYQ29 (unpublished plasmid from Y.
170 Gao), resulting in strain TNVS608 (*P_{xyl}-sftA*). Subsequently, TNVS608 was transformed with
171 chromosomal DNA from either strain PG62 (*P_{spac}-yfp-ftsA*) (Gamba *et al.*, 2009), PG227
172 (*P_{spac}-yfp-pbpB*) (Gamba *et al.*, 2009) or YK203 (*P_{spac}-yfp-sepF*) (Ishikawa *et al.*, 2006),
173 resulting in strains TNVS650, TNVS652 and TNVS708, respectively. These strains were
174 subsequently transformed with chromosomal DNA from strain LH028 (*ezrA::cat*) (Gamba *et*

175 *al.*, 2015), resulting in the final test strains TNVS650, TNVS652 and TNVS708, respectively.

176 To test the effect of *sftA* and *sepF* deletions on chromosome bisection, strains
177 TNVS371 (*yneABC::tet*), TNVS089 (*sftA::erm yneABC::tet*), TNVS373 (*sepF::spc yneABC::tet*)
178 and TNVS431 (*sftA::erm sepF::spc yneABC::tet*) were created by transforming genomic DNA
179 of strain YK138 (Bohorquez *et al.*, 2018) into strains *B. subtilis* 168, TNVS083 (*sftA::erm*),
180 TNVS159 (*sepF::spc*) and TNVS152 (*sftA::erm sepF::spc*), respectively.

181 To quantify FtsZ-rings formation over nucleoids strain TNVS354 (*chr::Pxyl-mCherry-*
182 *zapA sftA::erm*) was constructed by transforming strain EKB036 (kind gift from Edward de
183 Koning) with chromosomal DNA from TNVS083.

184

185 **Table S1. *B. subtilis* trains used in this study.**

strain	genotype	reference
168	<i>trpC2</i>	(Zeigler <i>et al.</i> , 2008)
DS7996	<i>lacA::lacI-tet amyE::lacZ-cat</i>	(Pozsgai <i>et al.</i> , 2011)
BKE29805	<i>sftA::erm</i>	(Koo <i>et al.</i> , 2017)
BKK29805	<i>sftA::kan</i>	(Koo <i>et al.</i> , 2017)
BFA2863	<i>sepF::erm</i>	(Hamoen <i>et al.</i> , 2006)
3294	<i>chr::P_{divIVA}-gfp-divIVA - cat chr::(P_{spac}-pbpB neo)</i>	(Hamoen and Errington, 2003)
1801	<i>chr::(P_{spac}-ftsZ ble)</i>	(Marston <i>et al.</i> , 1998)
1356	<i>zapA-yshB::tet</i>	(Feucht and Errington, 2005)
EKB036	<i>chr::(P_{xyI}-mCherry-zapA-cat)</i>	Gift from E. de Koning unpublished
TB07	<i>ftsA::erm</i>	This work
LH028	<i>ezrA::cat</i>	(Gamba <i>et al.</i> , 2015)
PG049	<i>ezrA::spc</i>	(Gamba <i>et al.</i> , 2015)
PG062	<i>aprE3'-spc-P_{spac}-yfp-ftsA-aprE5'</i>	(Gamba <i>et al.</i> , 2009)
PG227	<i>aprE3'-spc-P_{spac}-yfp-pbpB-aprE5'</i>	(Gamba <i>et al.</i> , 2009)
TNVS001	<i>amyE3'-spc-P_{xyI}-sftA-gfp-amyE5'</i>	This work
TNVS042	<i>amyE3'-P_{xyI}-mgfp-ydeL-amyE5'</i>	This work
TNVS083	<i>sftA::erm</i> (BKE29805 transformed to 168)	This work
TNVS087	<i>chr::(P_{spac}-pbpB neo)</i> (3294 transformed to 168)	This work
TNVS089	<i>sftA::erm yneABC::tet</i>	This work
TNVS152	<i>sftA::erm sepF::spc</i>	This work
TNVS158	<i>ezrA::spc</i> (PG049 transformed to 168)	This work
TNVS159	<i>sepF::spc</i> (YK204 transformed to 168)	This work
TNVS171	<i>sftA::erm ezrA::spc</i>	This work
TNVS193	<i>zapA::tet</i> (1356 transformed to 168)	This work
TNVS197	<i>sftA::erm zapA::tet</i>	This work
TNVS209	<i>lacA::lacI-tet</i> (DS7996 transformed to 168)	This work
TNVS224	<i>amyE3'-spc-P_{xyI}-sftA(M1-P149)Δ(Q30-R75)-mgfp-amyE5'</i>	This work
TNVS234	<i>sftA::erm amyE3'-spc-P_{xyI}-sftA(M1-P149)Δ(Q30-R75)-mgfp-amyE5'</i>	This work
TNVS248	<i>ydeL::erm</i> (BKE05240 transformed to 168)	This work
TNVS254	<i>amyE3'-spc-P_{xyI}-sftA-mgfp-amyE5' sftA::erm ylmFGH::kan</i>	This work
TNVS281	<i>ftsA::erm P_{spac}-ftsZ</i> (YK206 transformed to 168)	This work
TNVS330	<i>amyE3'-spc-P_{xyI}-sftA-mgfp-amyE5' ftsA::erm</i>	This work
TNVS342	<i>amyE3'-spc-P_{xyI}-sftA-mgfp-amyE5' zapA::tet</i>	This work
TNVS343	<i>amyE3'-spc-P_{xyI}-sftA-mgfp-amyE5' ezrA::tet</i>	This work
TNVS353	<i>chr::(P_{xyI}-mCherry-zapA-cat) amyE3'-spc-P_{xyI}-sftA-mgfp-amyE5'</i>	This work
TNVS366	<i>amyE3'-P_{xyI}-mgfp-ydeL-amyE5' ydeL::erm</i>	This work
TNVS371	<i>yneABC::tet</i> (YK138 transformed to 168)	This work
TNVS373	<i>yneABC::tet sepF::spc</i>	This work
TNVS390	<i>amyE3'-spc-P_{xyI}-sftA-amyE5'</i>	This work
TNVS431	<i>yneABC::tet sepF::spc sftA::erm</i>	This work
TNVS456	<i>sftA::erm amyE3'-spc-P_{xyI}-sftA(M1-P149)-mgfp-amyE5</i>	This work
TNVS541	<i>amyE3'-spc-P_{xyI}-sftA(M1-P149)-His6-amyE5'</i>	This work
TNVS586	<i>amyE3'-spc-P_{xyI}-sftA (M1-E14)-mgfp-amyE5'</i>	This work
TNVS591	<i>amyE3'-spc-P_{xyI}-sftA-amyE5' ezrA::cat</i>	This work
TNVS602	<i>amyE3'-spc-P_{xyI}-sftA(M1-P149)-2GS-His6-amyE5' ezrA::cat</i>	This work
TNVS605	<i>amyE3'-spc-P_{xyI}-sftA-amyE5' sepF::erm</i>	This work
TNVS606	<i>amyE3'-spc-P_{xyI}-sftA-amyE5' zapA::tet</i>	This work
TNVS608	<i>amyE3'-spc::kan-P_{xyI}-sftA-amyE5'</i>	This work
TNVS622	<i>amyE3'-spc-P_{xyI}-sftA-amyE5' ftsA::erm</i>	This work
TNVS650	<i>amyE3'-kan-P_{xyI}-sftA-amyE5'- aprE3'-spc-P_{spac}-yfp-ftsA-aprE5'</i>	This work
TNVS652	<i>amyE3'-kan-P_{xyI}-sftA-amyE5'- aprE3'-spc-P_{spac}-yfp-sepF-aprE5'</i>	This work
TNVS708	<i>amyE3'-kan-P_{xyI}-sftA-amyE5'- aprE3'-spc-P_{spac}-yfp-pbpB-aprE5'</i>	This work

TNVS710	<i>amyE3'-kan-P_{xyI}-sftA-amyE5'- aprE3'-spc-P_{spac}-yfp-ftsA-aprE5' ezrA::cat</i>	This work
TNVS712	<i>amyE3'-kan-P_{xyI}-sftA-amyE5'- aprE3'-spc-P_{spac}-yfp-sepF-aprE5' ezrA::cat</i>	This work
TNVS713	<i>amyE3'-kan-P_{xyI}-sftA-amyE5'- aprE3'-spc-P_{spac}-yfp-pbpB-aprE5' ezrA::cat</i>	This work
TNVS729	<i>amyE3'-spc-P_{xyI}-sftAΔ(S2-L12)-4GS-msfGFP-His6-amyE5'</i>	This work
TNVS758	<i>chr:::(P_{xyI}-mCherry-zapA-cat) cat amyE3'-spc-P_{xyI}-sftA-mgfp-amyE5' lacA::lacI-tet</i>	This work
TNVS776	<i>psdS::erm (BKE34710 transform to 168)</i>	This work
TNVS783	<i>chr:::(P_{xyI}-mCherry-zapA-cat) amyE3'-spc-P_{xyI}-sftA-mgfp-amyE5' lacA::lacI-tet chr:::(P_{spac}-pbpB-neo)</i>	This work
TNVS786	<i>chr:::(P_{xyI}-mCherry-zapA-cat) amyE3'-spc-P_{xyI}-sftA-mgfp-amyE5' lacA::lacI-tet chr:::(P_{spac}-ftsZ ble)</i>	This work
TNVS810	<i>amyE3'-spc-P_{xyI}-psdS-mgfp-amyE5'</i>	This work
TNVS825	<i>sftA::kan (BKK29805 transformed to 168)</i>	This work
TNVS947	<i>amyE3'-spc-P_{xyI}-sftAΔ(S2-L12)-amyE5' sftA::kan</i>	This work
TNVS949	<i>amyE3'-spc-P_{xyI}-sftAΔ(S2-L12)-amyE5' sftA::kan ΔsepF::erm</i>	This work
TNVS950	<i>amyE3'-spc-P_{xyI}-sftAΔ(S2-L12)-amyE5' sftA::kan ΔftsA::erm</i>	This work
TNVS951	<i>amyE3'-spc-P_{xyI}-sftAΔ(S2-L12)-amyE5' sftA::kan ΔezrA::cat</i>	This work
TNVS952	<i>amyE3'-spc-P_{xyI}-sftAΔ(S2-L12)-amyE5' sftA::kan ΔzapA::tet</i>	This work
TZH010	<i>amyE3'-spc-P_{xyI}-msfgfp-sftAΔ(M1-E250)-amyE5'</i>	This work
TZH018	<i>amyE3'-spc-P_{xyI}-msfgfp-sftAΔ(M1-E250)-amyE5' sftA::kan sepF::erm</i>	This work
TZH021	<i>amyE3'-spc-P_{xyI}-msfgfp-sftAΔ(M1-E250)-amyE5' sftA::kan</i>	This work
TZH022	<i>amyE3'-spc-P_{xyI}-msfgfp-sftAΔ(M1-E250)-amyE5' sftA::kan ftsA::cat</i>	This work
TZH029	<i>amyE3'-spc-P_{xyI}-sftA(M1-P61)-msfgfp-amyE5'</i>	This work
TZH035	<i>amyE3'-spc-P_{xyI}-sftA(M1-P61)-msfgfp-amyE5' sftA::kan</i>	This work
TZH051	<i>amyE3'-spc-P_{xyI}-sftA(M1-P61)-msfgfp-amyE5' sftA::kan ftsA::cat</i>	This work
TZH053	<i>amyE3'-spc-P_{xyI}-sftA(M1-P61)-msfgfp-amyE5' sftA::kan sepF::erm</i>	This work
TZH119	<i>amyE3'-spc-P_{xyI}-sftA(M1-P61)-msfgfp-amyE5' chr:::(P_{xyI}-mCherry-zapA-cat) sftA::kan</i>	This work
TZH120	<i>amyE3'-spc-P_{xyI}-sftA(M1-P61)-msfgfp-amyE5' chr:::(P_{xyI}-mCherry-zapA-cat) sftA::kan ftsA::erm</i>	This work
TZH121	<i>amyE3'-spc-P_{xyI}-sftA(M1-P61)-msfgfp-amyE5' chr:::(P_{xyI}-mCherry-zapA-cat) sftA::kan sepF::erm</i>	This work
YK138	<i>yneABC::tet</i>	(Bohorquez <i>et al.</i> , 2018)
YK203	<i>aprE3'-spc-P_{spac}-yfp-yImF-aprE5'</i>	(Ishikawa <i>et al.</i> , 2006)
YK204	<i>sepF::spc</i>	(Ishikawa <i>et al.</i> , 2006)
YK206	<i>ftsA::erm P_{spac}-ftsZ</i>	(Ishikawa <i>et al.</i> , 2006)
GYQ300	<i>ftsA::cat</i>	Kind gift of Y. Gao

186 *gfp*, *mgfp* and *msfgfp* indicate green fluorescent protein (GFP), the monomeric and
187 monomeric super folder variants, respectively. *tet*, *cat*, *spec* and *erm* indicate tetracycline,
188 chloramphenicol, spectinomycin and erythromycin resistance cassettes, respectively.

189 **Table S2. Plasmids used in this study.**

plasmid	relevant genotype	reference
pET24A	<i>lacI-T₇-lacO-kan</i>	Novagen
pMW1*	<i>amyE3'-spc-P_{xyI}-MCS-msfgfp-amyE5' bla</i>	(Müller <i>et al.</i> , 2016)
pNC12	<i>P_{tac}-malE-sepF</i>	(Duman <i>et al.</i> , 2013)
pSEN29	<i>bla Rep101 pSC101 ori</i>	(Genevaux <i>et al.</i> , 2004)
pSG1154	<i>amyE3'-spc-P_{xyI}-mcs-gfp-amyE5' bla</i>	(Lewis and Marston, 1999)
pSG1729	<i>amyE3'-spc-P_{xyI}-gfp-mcs-amyE5' bla</i>	(Lewis and Marston, 1999)
pTNV001	<i>amyE3'-spc-P_{xyI}-sftA-gfp-amyE5' bla</i>	This work
pTNV022	<i>amyE3'-spec-P_{xyI}-mgfp-ydeL-amyE5' bla</i>	This work
pTNV061	<i>amyE3'-spec-P_{xyI}-MCS-amyE5' bla</i>	This work
pTNV063	<i>amyE3'-spc-P_{xyI}-sftA-msfgfp-amyE5' bla</i>	This work
pTNV064*	<i>amyE3': spec-P_{xyI}-MCS-msfgfp-amyE5' bla</i>	This work
pTNV069	<i>amyE3': spec-P_{xyI}-sftA(M1-P149)-msfgfp-amyE5' bla</i>	This work
pTNV082	<i>lacI-T₇-lacO-sftA-His₆-kan</i>	This work
pTNV093	<i>amyE3': spec-P_{xyI}-sftA(M1-P149)Δ(Q30-R75)-mgfp-amyE5' bla</i>	This work
pTNV100	<i>amyE3'-spec-P_{xyI}-msfgfp-MCS-amyE5' bla</i>	This work
pTNV122	<i>amyE3'-spec-P_{xyI}-MCS-amyE5' bla Rep101 pSC101 ori</i>	This work
pTNV124	<i>amyE3': spec-P_{xyI}-sftA(M1-P149)-msfgfp-His₆-amyE5' bla</i>	This work
pTNV125	<i>amyE3'-spec-P_{xyI}-sftA-amyE5' bla Rep101 pSC101 ori</i>	This work
pTNV143	<i>amyE3': spec-P_{xyI}-msfgfp-His₆-amyE5' bla</i>	This work
pTNV144	<i>amyE3'-spc-P_{xyI}-sftA-msfgfp-His₆-amyE5' bla</i>	This work
pTNV166	<i>amyE3': spec-P_{xyI}-sftA(M1-P149)-His₆-amyE5' bla</i>	This work
pTNV187	<i>amyE3': spec-P_{xyI}-sftA(M1-E14)-His₆-amyE5' bla</i>	This work
pTNV202	<i>amyE3': spec-P_{xyI}-sftAΔ(S2-L12)-msfgfp-His₆-amyE5' bla</i>	This work
pZH008	<i>amyE3'-spc-P_{xyI}-msfgfp-sftAΔ(M1-E250)-amyE5' bla</i>	This work
pZH014	<i>amyE3'-spc-P_{xyI}-sftA(M1-P61)-msfgfp-amyE5' bla</i>	This work
pYQ29	<i>spc::kan bla</i>	Kind gift of Y. Gao

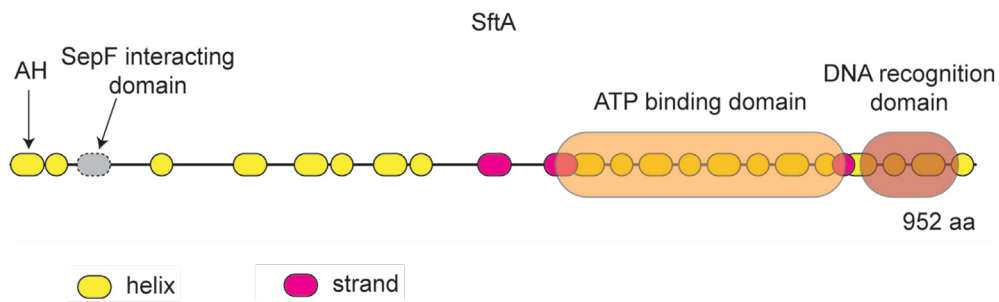
190 * the MCS of plasmid pMW1 adds two amino acids to the fused protein.

191 *gfp*, *mgfp* and *msfgfp* indicate green fluorescent protein (GFP), the monomeric and
 192 monomeric super folder variants, respectively. *tet*, *cat*, *spec* and *erm* indicate tetracycline,
 193 chloramphenicol, spectinomycin and erythromycin resistance cassettes, respectively. *mcs*
 194 indicates multiple cloning site.

primer	sequence 5'→3'
AH001	GGCTCAGGAAGCCATCATCACCATCACCCTAG
AH002	TGATGATGGCTTCTGAGCCCGTTCTTCAATGTTTCAGAAGGCT
TerS001	GGGGGGGGGCCCATGAGTTGGCTTCATAAAT
TerS002	CCCCGAATTCGATCCTGAGCCGCTTCTGAGCCTTCGTTTATTAATCAC
TerS127	GGGCTCGAGGGCTCAGGAAGCGGCTCAGGATCCGATATCACGCCTTTTTGAATAGA
TerS128	CCCGCGGCCGCCTCATATCTTCCAGGCAGCCTTCA
TerS145	ATAAACAAATAGGGGTTCCGCGCA
TerS146	TGCGCGGAACCCCTATTTGTTTAT
TerS153	GGCTCAGGAAGCGGCTCAGGATCCAGTAAAGGAGAAGAACT
TerS179	CGCACACCATCGGACGAACCGA
TerS180	GGTTCGTCCGATGGTGTGCGCGGAATTTGAGCGGGTTTTGTCT
TerS203	CCTGAGCCGCTTCTGAGCCCGTTCTGTTCAATGTTTCA
TerS226	GGGGAAGGCCATCCAGCCTCGCGT
TerS261	TGGATCCGAAGTCTGGACATCTGCAGGGTACCCATCCTAGGA
TerS262	ATGTCCAGACTTCGGATCCA
TerS263	CAATTCTAGTTCTAGAGCGGCCGCGA
TerS274	CATCCTAGGAATCTCCTTTCTAGA
TerS279	GAAAGGAGATTCTAGGATGAGTTGGCTTCATAAATTTTTTGA
TerS280	CCTGAGCCGCTTCTGAGCCTTCGTTTATTAATCACTTGCT
TerS282	GAAAGGAGATTCTAGGATGGGCGAAAGCGAAGAGGATGCTGA
TerS283	TTTGTAGAGCTCATCCATGCCATGTGT
TerS287	CTGTAGACAAATTGTGAAAGGAT
TerS341	CGCGGTCATCAATCATACCACCA
TerS342	TGGTATGATTGATGACCGCGTCA
TerS357	CCGCTCTAGAAGTAGAATTGTTATTCGTTTATTAATCACTTGCTGTGA
TerS368	GGCTCAGGAAGCGGCTCAGGATCCAAAGGAGAAGAACTTTTCACTGGAGT
TerS382	CAAAAAGGATCTTACCTAGATCCT
TerS413	GAAAGGAGATTCTAGGATGAGCAAAGGAGAAGAACTTTTCACT
TerS414	GCATGGATGAGCTCTACAAAGGCTCAGGAAGCGGCTCAGGATCCTCCAGACTTCGGATCCACGGGCCCCCCCT
TerS478	AGGATCTAGGTGAAGATCCTTTTTGCACCGTTTTTTCATCTGTGCATATGGA
TerS479	CGCGACGCGAGGCTGGATGGCCTTCCCCAT
TerS484	GGCATGGATGAGCTCTACAAAGGCTCAGGAAGCCATCATCACCATCACCCTAGATGTCCAGACTTCAGATCCA
TerS573	CCTGAGCCGCTTCTGAGCCTTCGCCTAAAAACAAATCAAAAAATTTATGAAGCCA
TerS621	GAAAGGAGATTCTAGGATGTTAAAGACTTATCTCATCGACCGCT
TerS622	CCTGAGCCGCTTCTGAGCCCAATGCTGTACATTACAGAGGGTGT
ZT059	AAGGCTCAGGAAGCGGCTCAATGCTCACAGATACGGCGGC
ZT060	AGCTTATCGATACCGTCGACTTATTCGTTTATTAATCACTTGCTGTG
ZT088	TCTAGAAAGGAGATTCTAGGATGAGTTGGCTTCATAAATTTTTGATTG
ZT089	ATTGAGCCGCTTCTGAGCCTGGAAAACGGAATTTGCCTTTTG
ZT189	CCTAGGAATCTCCTTTCTAGATGC
ZT200	TGAGCCGCTTCTGAGCCTTTGTAGAGCTCATCCATGCC
EKP22	GTCGACGGTATCGATAAGCTTGAT

197 **Fig. S1**

198



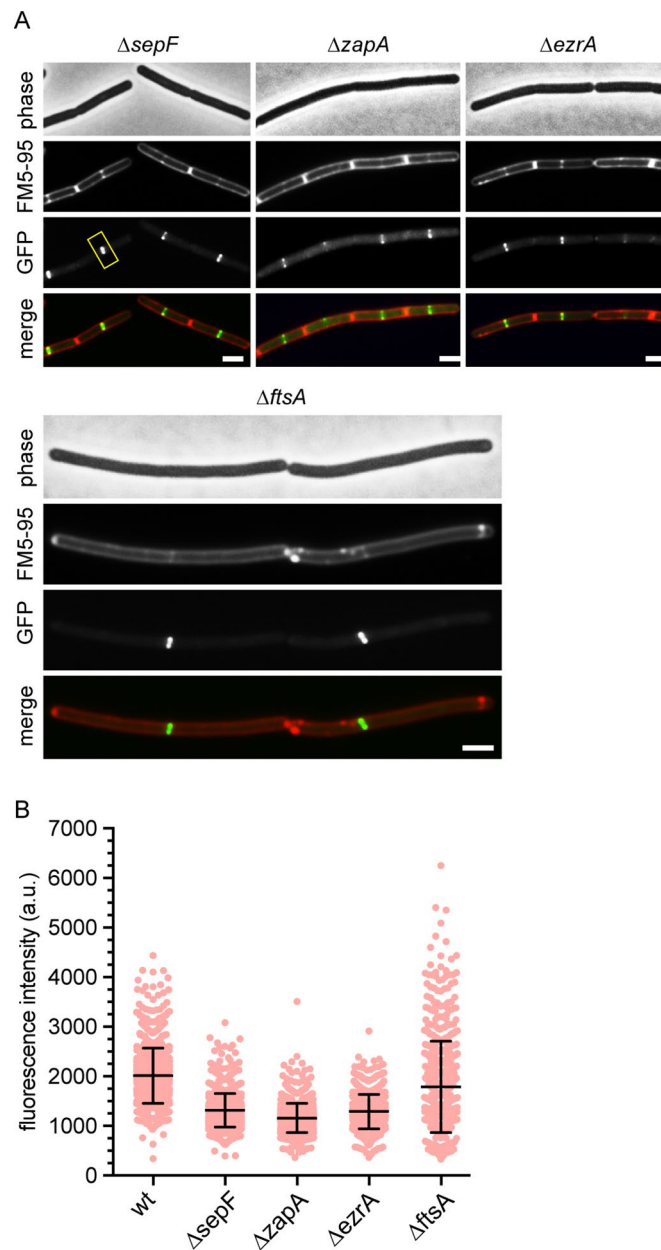
199

200

201 **Fig. S1 Secondary structure prediction of SftA using PSIPred.**

202 Secondary structure analysis was performed using PSIPred (Jones et al. 1999). The cartoon
203 depicts the main predicted alpha helices (helix), beta strands (strand) and the putative ATP
204 binding domain and DNA binding domain of SftA. The putative SepF interacting domain of
205 SftA (amino acids P61-R75) found in the yeast two-hybrid analysis is indicated in grey, and
206 the membrane-binding amphipathic helix is indicated as AH.

207



209

210

211 **Fig. S2. Localization of SftA in different cell division mutants.**

212 (A) Fluorescence microscopy images of SftA-GFP in different *B. subtilis* cell division mutants.

213 SftA-GFP expression was induced with 0.1 % xylose. Membranes were stained with FM5-95.

214 Scale bars are 2 μ m. (B) Scatter plot indicating the SftA-GFP fluorescence intensities at cell

215 division sites (yellow box in A) of the different mutants. On average 500 cells were measured.

216 Strains used: TNVS001, TNVS254, TNVS342, TNVS343 and TNVS330, respectively.

217

218 **Fig. S3**

219

220

221

222

223

224

225

226

227

228

229

230

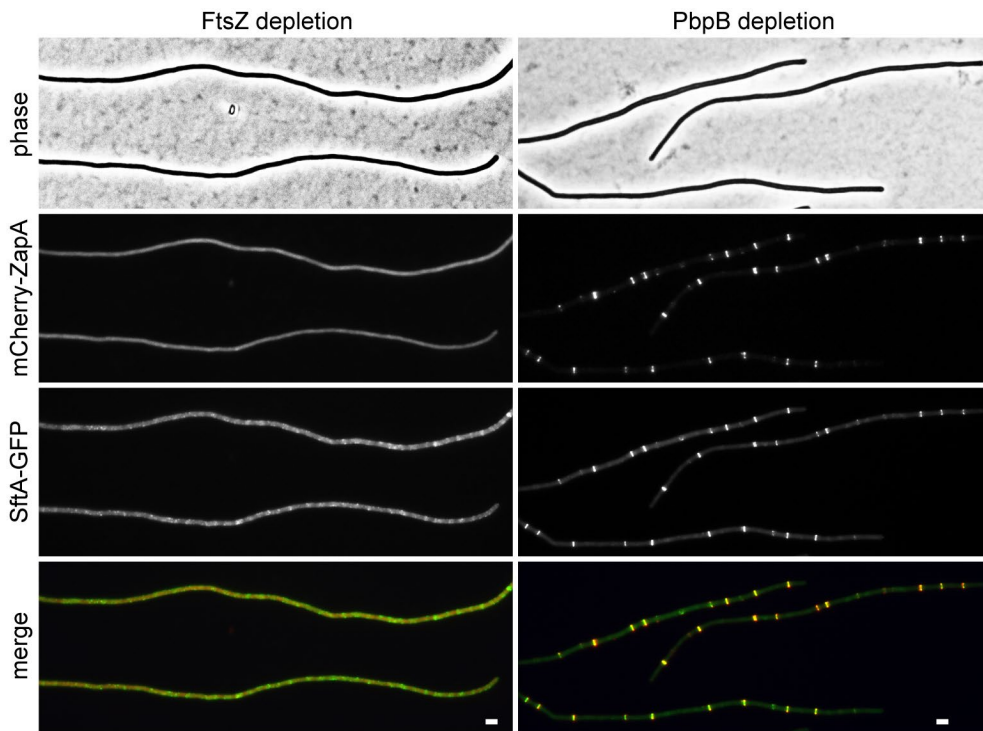
231

232

233

234

235



236 **Fig. S3. SftA recruitment does not depend on late cell division proteins.**

237 Localization of SftA-GFP and mCherry-ZapA in cells containing either an IPTG-inducible *ftsZ*

238 (left panels) or *pbp2B* gene (right panels). Cells were grown for 3 h in the absence of IPTG

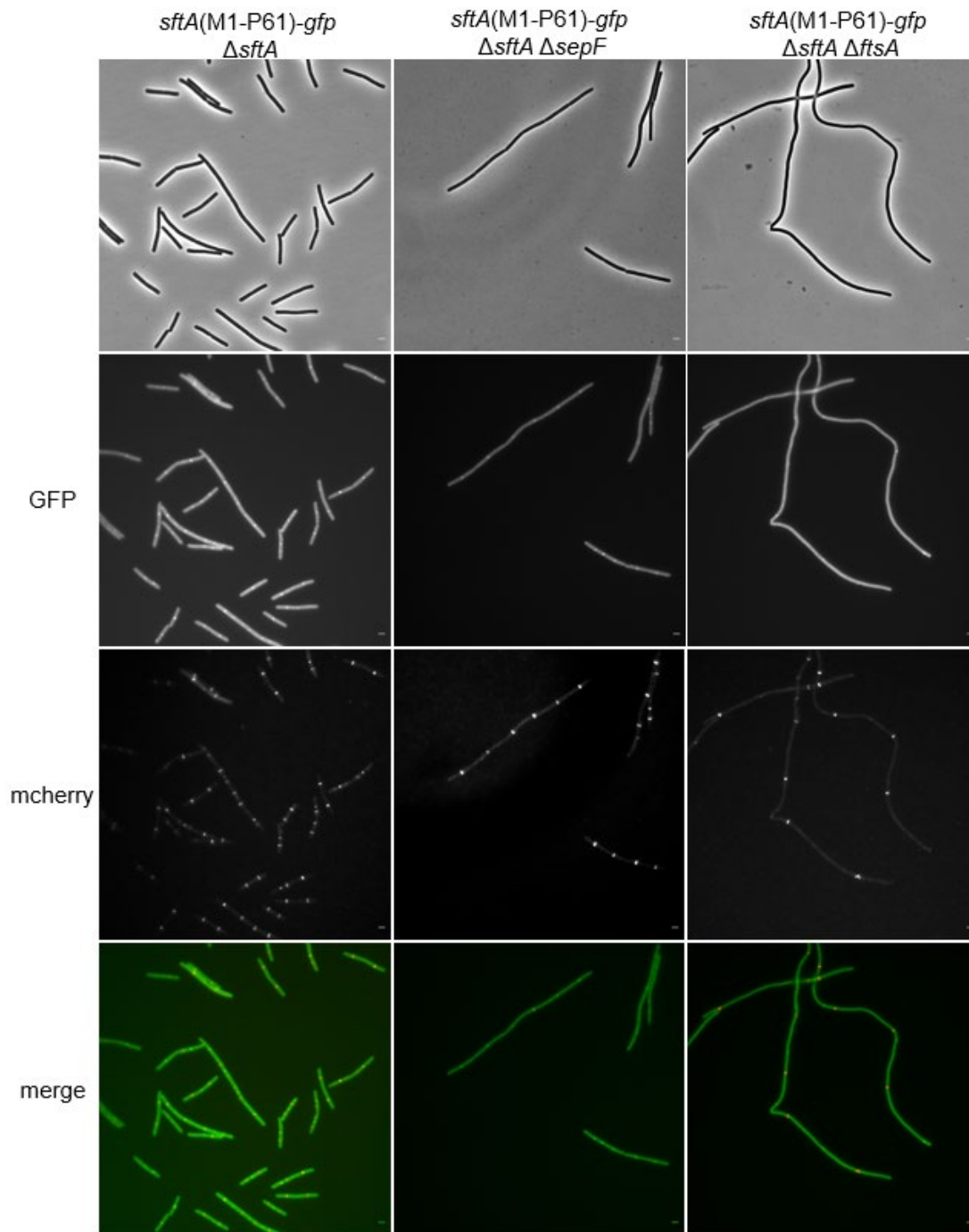
239 resulting in filamentation. In the absence of Pbp2B, Z-rings are still being formed. SftA-GFP

240 and mCherry-ZapA were induced with 0.1 % xylose. Scale bars are 2 μ m. Strains used:

241 TNVS783 and TNVS786, respectively.

242

243 **Fig. S4**
244



273

274 **Fig. S4. Large field microscopy images of mutants shown in Fig. 5.**

275 Large field images related to main text Fig. 5. Localization of GFP fused to the first 61 amino
276 acids of SftA (green) in different *B. subtilis* mutants. All strains lacked wild type *sftA*, and all
277 strains contained an mCherry-ZapA fusion (red) to indicate the localization of Z-rings.
278 Expression of the fusion proteins was induced with 0.1 % xylose. Scale bars are 2 μm. Strains
279 used, TZH029, TZH119, TZH120, TZH121, respectively.

280 **Fig. S5**

281

282

283

284

285

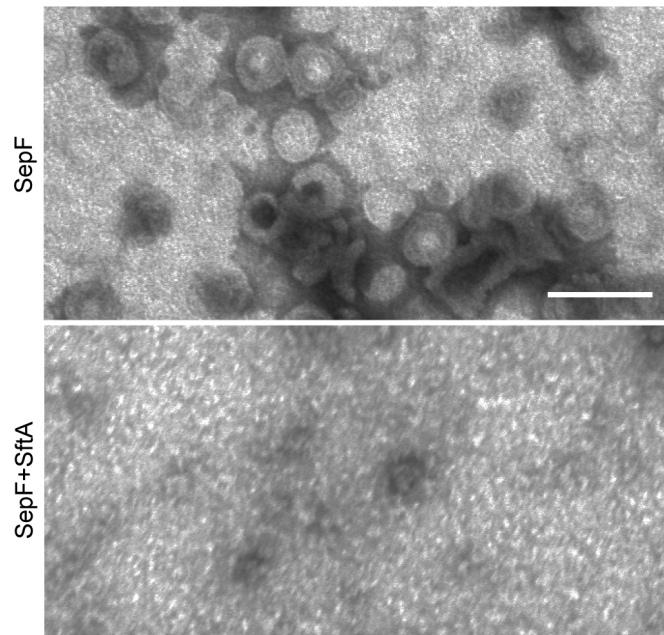
286

287

288

289

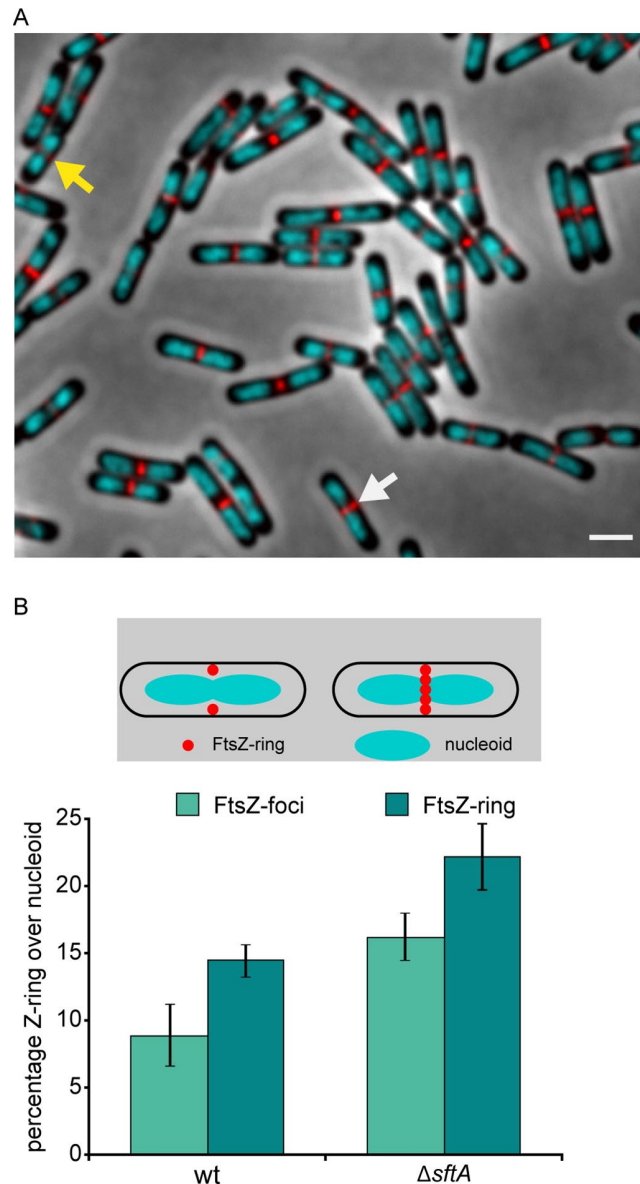
290



291 **Fig. S5. SftA inhibits SepF ring formation.**

292 SepF forms large protein rings with a diameter of approximately 50 nm (top EM image), after
293 cleavage of the MBP (Maltose binding protein) moiety from the purified MBP-SepF fusion by
294 factor Xa. The formation of these rings is inhibited when the cleavage reaction is carried out
295 in the presence of SftA at a molar ratio of MBP-SepF:SftA of 3:1. Scale bar is 100 nm.

296



298

299 **Fig. S6. Assembly of FtsZ-rings over nucleoids.**

300 (A) $\Delta sftA$ cells expressing mCherry-ZapA (red) as FtsZ-ring marker with nucleoids (turquoise)
 301 stained with DAPI. The start of a Z-ring can be observed in microscopic images by the
 302 formation of two opposite red fluorescence foci at midcell (yellow arrow). Over time the Z-
 303 ring becomes more intense and septum synthesis begins resulting in a clear fluorescent band
 304 (white arrow) that eventually becomes smaller, since the Z-ring forms the leading edge of the
 305 closing septal wall. Scale bar is 2 μ m. (B) Bar diagram indicating the average localization of
 306 early FtsZ foci and Z-rings over nucleoids, based on 3 independent biological experiments
 307 (approximately 100 cells counted). Cartoon above the bar diagram illustrates how FtsZ-rings
 308 over nucleoids were scored. Standard errors are indicated. Strains used: TNVS354 and
 309 EKB036.

310 **References**

311

312 Bohorquez, L.C., Surdova, K., Jonker, M.J., and Hamoen, L.W. (2018) The Conserved DNA
313 Binding Protein WhiA Influences Chromosome Segregation in *Bacillus subtilis*. *J Bacteriol*
314 200.

315 Duman, R., Ishikawa, S., Celik, I., Strahl, H., Ogasawara, N., Troc, P., *et al.* (2013) Structural
316 and genetic analyses reveal the protein SepF as a new membrane anchor for the Z ring. *Proc*
317 *National Acad Sci* 110: E4601–E4610.

318 Feucht, A., and Errington, J. (2005) *ftsZ* mutations affecting cell division frequency,
319 placement and morphology in *Bacillus subtilis*. *Microbiology+* 151: 2053–2064.

320 Gamba, P., Rietkötter, E., Daniel, R.A., and Hamoen, L.W. (2015) Tetracycline
321 hypersensitivity of an *ezrA* mutant links GalE and TseB (YpmB) to cell division. *Front*
322 *Microbiol* 6: 346.

323 Gamba, P., Veening, J.-W., Saunders, N.J., Hamoen, L.W., and Daniel, R.A. (2009) Two-Step
324 Assembly Dynamics of the *Bacillus subtilis* Divisome. *J Bacteriol* 191: 4186–4194.

325 Genevoux, P., Keppel, F., Schwager, F., Langendijk-Genevoux, P.S., Hartl, F.U., and
326 Georgopoulos, C. (2004) In vivo analysis of the overlapping functions of DnaK and trigger
327 factor. *Embo Rep* 5: 195–200.

328 Gibson, D.G., Young, L., Chuang, R.-Y., Venter, J.C., Hutchison, C.A., and Smith, H.O. (2009)
329 Enzymatic assembly of DNA molecules up to several hundred kilobases. *Nat Methods* 6:
330 343–345.

331 Hamoen, L.W., and Errington, J. (2003) Polar Targeting of DivIVA in *Bacillus subtilis* Is Not
332 Directly Dependent on FtsZ or PBP 2B. *J Bacteriol* 185: 693–697.

333 Hamoen, L.W., Meile, J., Jong, W.D., Noirot, P., and Errington, J. (2006) SepF, a novel FtsZ-
334 interacting protein required for a late step in cell division. *Mol Microbiol* 59: 989–999.

335 Ishikawa, S., Kawai, Y., Hiramatsu, K., Kuwano, M., and Ogasawara, N. (2006) A new FtsZ-
336 interacting protein, YlmF, complements the activity of FtsA during progression of cell
337 division in *Bacillus subtilis*. *Mol Microbiol* 60: 1364–1380.

338 Jones, D.T. (1999) Protein secondary structure prediction based on position-specific scoring
339 matrices1 1Edited by G. Von Heijne. *J Mol Biol* 292: 195–202.

340 Koo, B.-M., Kritikos, G., Farelli, J.D., Todor, H., Tong, K., Kimsey, H., *et al.* (2017) Construction
341 and Analysis of Two Genome-Scale Deletion Libraries for *Bacillus subtilis*. *Cell Syst* 4: 291-
342 305.e7.

343 Lewis, P.J., and Marston, A.L. (1999) GFP vectors for controlled expression and dual labelling
344 of protein fusions in *Bacillus subtilis*. *Gene* 227: 101–109.

- 345 Marston, A.L., Thomaidis, H.B., Edwards, D.H., Sharpe, M.E., and Errington, J. (1998) Polar
346 localization of the MinD protein of *Bacillus subtilis* and its role in selection of the mid-cell
347 division site. *Gene Dev* 12: 3419–3430.
- 348 Müller, A., Wenzel, M., Strahl, H., Grein, F., Saaki, T.N.V., Kohl, B., *et al.* (2016) Daptomycin
349 inhibits cell envelope synthesis by interfering with fluid membrane microdomains. *Proc*
350 *National Acad Sci* 113: E7077–E7086.
- 351 Pozsgai, E.R., Blair, K.M., and Kearns, D.B. (2011) Modified mariner Transposons for Random
352 Inducible-Expression Insertions and Transcriptional Reporter Fusion Insertions in *Bacillus*
353 *subtilis*. *Appl Environ Microb* 78: 778–785.
- 354 Zeigler, D.R., Prágai, Z., Rodriguez, S., Chevreux, B., Muffler, A., Albert, T., *et al.* (2008) The
355 Origins of 168, W23, and Other *Bacillus subtilis* Legacy Strains. *J Bacteriol* 190: 6983–6995.
- 356